The theoretical prediction for the muon anomalous magnetic moment

M. Davier, W.J. Marciano

The theoretical prediction for the muon anomalous magnetic moment

MICHEL DAVIER[a] AND WILLIAM J. MARCIANO[b]

[a] *Laboratoire de l'Accélérateur Linéaire, IN2P3-CNRS et Université de Paris Sud, 91898 Orsay, France*

[b] *Brookhaven National Laboratory, Upton, NY 11973*

Key Words muon, magnetic moment, quantum electrodynamics, electroweak theory, vacuum polarization, spectral functions

Abstract The Standard Model prediction for the muon anomalous magnetic moment is reviewed. Recent updates of QED, electroweak and hadronic contributions are described. Comparison of theory and experiment suggests a 2.4 σ difference if $e^+e^- \to$ hadrons data are used to evaluate the main hadronic effects, but a smaller discrepancy if hadronic τ decay data are employed. Implications of a deviation for "new physics" contributions along with an outlook for future improvements in theory and experiment are briefly discussed.

CONTENTS

1 INTRODUCTION

One of the great successes of the Dirac equation (1) was its prediction that the magnetic dipole moment, $\vec{\mu}$, of a spin $|\vec{s}| = 1/2$ particle such as the electron (or muon) is given by

$$\vec{\mu}_l = g_l \frac{e}{2m_l}\vec{s}, \qquad l = e, \mu \ldots \tag{1}$$

with gyromagnetic ratio $g_l = 2$, a value already implied by early atomic spectroscopy. Later it was realized that a relativistic quantum field theory such as quantum electrodynamics (QED) can give rise via quantum fluctuations to a shift in g_l

$$a_l \equiv \frac{g_l - 2}{2} \tag{2}$$

called the magnetic anomaly. In a now classic QED calculation, Schwinger (2) found the leading (one loop) effect (Fig. 1)

$$a_l = \frac{\alpha}{2\pi} \simeq 0.00116$$
$$\alpha \equiv \frac{e^2}{4\pi} \simeq 1/137.036 \qquad (3)$$

which agreed beautifully with experiment (3), thereby providing strong confidence in the validity of perturbative QED. Today, we continue the tradition of testing QED and its $SU(3)_C \times SU(2)_L \times U(1)_Y$ Standard Model (SM) extension (which includes strong and electroweak interactions) by measuring $a_l^{\rm exp}$ for the electron and muon ever more precisely and comparing with $a_l^{\rm SM}$ expectations, calculated to much higher order in perturbation theory. Such comparisons test the validity of the SM and probe for "new physics" effects, which if present in quantum loop fluctuations should cause disagreement at some level.

For the electron and positron (expected to have the same a_e if CPT symmetry holds), a series of (Nobel prize) experiments by Dehmelt and collaborators (4) found

$$a_{e^-}^{\rm exp} = 0.0011596521884(43) \ ,$$
$$a_{e^+}^{\rm exp} = 0.0011596521879(43) \ , \qquad (4)$$

where the bracketed number denotes the uncertainty in the last two significant figures. Those results are to be compared with the SM prediction (5, 6)

$$a_e^{\rm SM} = \frac{\alpha}{2\pi} - 0.328478444(\frac{\alpha}{\pi})^2 + 1.181234(\frac{\alpha}{\pi})^3 - 1.7502(\frac{\alpha}{\pi})^4 + 1.7 \times 10^{-12} \qquad (5)$$

where the last very small term stems from strong (hadronic) and electroweak quantum corrections (7) which are of order $\sim (\alpha/\pi)^2 \ (m_e/m_\rho)^2 \simeq 2 \times 10^{-12}$ and $\sim (\alpha/\pi) \ (m_e/m_W)^2 \simeq \ 10^{-13}$ respectively.

Comparison of Eqs. (4) and (5) yields the most precise determination of the fine structure constant (8)

$$\alpha^{-1} = 137.03599877(40) \ . \tag{6}$$

The agreement of that value with the more direct (but less precise) measurements (9) of α

$$\begin{aligned}
\alpha^{-1} &= 137.03600300(270) \qquad [\text{Quantum Hall}] \ , \\
\alpha^{-1} &= 137.03600840(330) \qquad [\text{Rydberg}(h/m_n)] \ , \\
\alpha^{-1} &= 137.03598710(430) \qquad [\text{AC Josephson}] \ , \\
\alpha^{-1} &= 137.03599520(790) \qquad [\text{Muonium HFS}] \ ,
\end{aligned} \tag{7}$$

confirms the validity of QED to a precision of 3×10^{-8}. That agreement along with other precision studies makes QED the best tested theory in physics. An experiment underway at Harvard (10) aims to improve the measurement of a_e by about a factor of 15. Combined with a much improved independent determination of α, it would significantly test the validity of perturbative QED (11). It should be noted, however, that a_e is in general not very sensitive to "new physics" at a high mass scale Λ because its effect on a_e is expected (12) to be quadratic in $1/\Lambda$

$$\Delta a_e(\Lambda) \sim \mathcal{O}(\frac{m_e^2}{\Lambda^2}) \tag{8}$$

and, hence, highly suppressed by the smallness of the electron mass. It would be much more sensitive if Δa_e were linear in $1/\Lambda$; but that is unlikely if chiral symmetry is present in the $m_e \to 0$ limit.

The muon magnetic anomaly has recently been measured with a precision of 5×10^{-7} by the E821 collaboration at Brookhaven National Laboratory (13).

$$a_{\mu^+}^{\rm exp} = 116592030(80) \times 10^{-11} \ ,$$

$$a_{\mu^-}^{\rm exp} = 116592140(85) \times 10^{-11} \ ,$$

$$a_{\mu}^{\rm exp} = 116592080(58) \times 10^{-11} \qquad [\text{average}] \ . \tag{9}$$

Although the accuracy is 200 times worse than $a_e^{\rm exp}$, a_μ is about $m_\mu^2/m_e^2 \simeq 40{,}000$ times more sensitive to "new physics" and hence a better place (by about a factor of 200) to search for a deviation from SM expectations. Of course, strong and electroweak contributions to a_μ are also enhanced by $m_\mu^2/m_e^2 \simeq 40{,}000$ relative to a_e; so, they must be evaluated much more precisely in any meaningful comparison of $a_\mu^{\rm SM}$ with Eq. (9). Fortunately, the recent experimental progress in $a_\mu^{\rm exp}$ has stimulated much theoretical improvement of $a_\mu^{\rm SM}$, uncovering errors and inspiring new computational approaches along the way.

The theoretical prediction for $a_\mu^{\rm SM}$ is generally divided into 3 contributions

$$a_\mu^{\rm SM} = a_\mu^{\rm QED} + a_\mu^{\rm EW} + a_\mu^{\rm hadronic} \tag{10}$$

and each has undergone and continues to be subjected to detailed scrutiny. The QED contribution has been computed through 4 loops (i.e. $\mathcal{O}(\alpha/\pi)^4$) and estimated at the 5-loop level. A recent (preliminary) revision (14) of the $(\alpha/\pi)^4$ contribution (described in Section 2 has shifted the prediction for $a_\mu^{\rm QED}$ up somewhat, by about 15×10^{-11}. Electroweak corrections have been computed at the one and two-loop levels (15), see Section 3. In fact $a_\mu^{\rm EW}$ represents the first full 2-loop EW Standard Model calculation. Hadronic (*i.e.* strong interaction) effects from low energy quark and gluon loop effects have been evaluated at order $(\alpha/\pi)^2$ and $(\alpha/\pi)^3$ using $e^+e^- \to$ hadrons data via a dispersion relation and employing hadronic τ decays as a consistency check. At the 3-loop level in α, the so-called hadronic light-by-light (LBL) contributions must be estimated in a model dependent approach. Those estimates have been plagued by errors which now seem to

be sorted out. Nevertheless, the remaining overall uncertainties from hadronic vacuum polarization and LBL in $a_\mu^{\rm hadronic}$ represent the main theoretical error in $a_\mu^{\rm SM}$. Its current status is reviewed in Sections 4 and 5.

In the remainder of this review, we describe the updates of QED, EW and hadronic contributions mentioned above, with particular emphasis on hadronic effects where the uncertainty is most problematic. We then compare (in Section 6) $a_\mu^{\rm exp}$ with $a_\mu^{\rm SM}$ and show that a 2.4 σ difference exists, using the estimate of $a_\mu^{\rm hadronic}$ from e^+e^- data. The implications of a deviation (if real) for "new physics" such as supersymmetry, extra dimensions, dynamical supersymmetry breaking etc. are very briefly outlined in Section 7. Finally, in Section 8 an outlook for possible future improvements in a_μ theory and experiment is given.

2 QED CONTRIBUTIONS

The QED contributions to $a_\mu^{\rm SM}$ start with $\alpha/2\pi$ from the Schwinger (2) one-loop diagram in Fig. 1 and include higher order extensions obtained by adding photon lines and closed lepton loops ($l = e, \mu, \tau$). Those contributions have been fully evaluated through 4 loops and the leading 5-loop effects (enhanced by $\ln(m_\mu/m_e) \sim 5.3$ factors) have been estimated (5, 6, 14, 16). Currently one finds

$$a_\mu^{\rm QED} = \frac{\alpha}{2\pi} + 0.765857376(\frac{\alpha}{\pi})^2 + 24.05050898(\frac{\alpha}{\pi})^3 + 131.0(\frac{\alpha}{\pi})^4 + 930(\frac{\alpha}{\pi})^5 \quad (11)$$

which for the value of α in Eq. (6) leads to

$$a_\mu^{\rm QED} = 116584720.7(0.4)(1) \times 10^{-11} \ . \quad (12)$$

That result is somewhat larger (by about 15×10^{-11}) than earlier predictions due to an update in the $(\frac{\alpha}{\pi})^4$ coefficient from 126 to a (preliminary) value of 131.0 reported by Kinoshita (14), and to a lesser extent, the small increase in α (see

Eq. (6)). The quoted errors in Eq. (12) stem from the uncertainties in α and the 5-loop QED estimate.

It is often noted that the coefficients in Eq. (11) are all positive and growing, whereas the coefficients in $a_e^{\rm SM}$ (see Eq. (5)) are better behaved, i.e. all of $O(1)$ and alternate in sign. That difference arises from electron vacuum polarization effects in $a_\mu^{\rm QED}$ (i.e. relatively large $\ln(m_\mu/m_e)$ contributions) and the unusually large contribution from the light-by-light scattering electron loop (16) which provides about 21 out of the 24 $\mathcal{O}(\alpha/\pi)^3$ coefficient. Once that coefficient turned out to be large and positive, the higher order coefficients were pretty much destined to be large and positive via electron vacuum polarization insertions in the light-by-light amplitudes. So the growing magnitude of the coefficients is well understood and not indicative of a breakdown in perturbation theory.

3 ELECTROWEAK CONTRIBUTIONS

Loop contributions to $a_\mu^{\rm SM}$ involving heavy $W^\pm$, Z or Higgs particles are collectively labeled as $a_\mu^{\rm EW}$. They are generically suppressed by a factor $(\alpha/\pi)(m_\mu/m_W)^2 \simeq 4\times10^{-9}$, but nevertheless within the sensitivity range of the E821 experiment (13). The one-loop contributions to $a_\mu^{\rm EW}$ illustrated in Fig. 2 were computed more than 30 years ago (17), primarily to test their finiteness (as required for renormalizability). Those studies found

$$\begin{aligned} a_\mu^{\rm EW,1-loop} &= \frac{G_\mu m_\mu^2}{8\sqrt{2}\pi^2}\left[\frac{5}{3}+\frac{1}{3}(1-4\sin^2\theta_W)^2+\mathcal{O}(\frac{m_\mu^2}{m_W^2})+\mathcal{O}(\frac{m_\mu^2}{m_H^2})\right] \\ G_\mu &= \frac{g^2}{4\sqrt{2}m_W^2} = 1.16637(1)\times10^{-5}\ {\rm GeV}^{-2} \\ \sin^2\theta_W &= 1-m_W^2/m_Z^2 = 0.223 \quad (\text{for } m_H = 150\ {\rm GeV}) \end{aligned} \tag{13}$$

or

$$a_\mu^{\rm EW,1-loop} = 194.8 \times 10^{-11} \ . \tag{14}$$

Interest in the 2-loop contribution to $a_\mu^{\rm EW}$ began with the observation (18) that some 2-loop EW diagrams containing photons and heavy weak bosons were enhanced by relatively large logs, $\ln(m_Z^2/m_\mu^2) \simeq 13.5$ relative to naive expectations. Later, the complete 2-loop calculation, including both logs and non-log parts was completed (15). Contributions enhanced by $\ln(m_Z/m_\mu)$ or $\ln(m_Z/m_f)$ $(m_f =$ fermion mass $\ll m_Z)$, called leading logs (LL), were recently updated and found to be (19)

$$a_\mu^{\rm EW,2-loop,LL} = \ -34.7(1.0) \times 10^{-11} \ , \tag{15}$$

while all other contributions, collectively called non-leading logs (NLL) give (15)

$$a_\mu^{\rm EW,2-loop,NLL} = \ -6.0(1.8) \times 10^{-11} \ , \tag{16}$$

where the uncertainty in Eq. (15) comes from hadronic effects in the quark triangle diagrams of Fig. 3 while the error in Eq. (16) stems mainly from the Higgs mass uncertainty. Together, they give

$$a_\mu^{\rm EW} = \ -\ 40.7(1.0)(1.8) \times 10^{-11} \ , \tag{17}$$

or combined with Eq. (14)

$$a_\mu^{\rm EW} = 154(1)(2) \times 10^{-11} \ . \tag{18}$$

The 21% reduction of the one-loop result is surprisingly large. Hence, it was important to evaluate the leading-log 3-loop effects of the form $G_\mu m_\mu^2 (\alpha/\pi)^2 (\ln(m_Z/m_\mu))^2$ via a renormalization group analysis. Such an analysis (19,20) found those effects to be negligibly small, $O(10^{-12})$.

Among the novel features of the full 2-loop EW calculation, the fermion triangle diagrams (Fig. 3) are perhaps the most interesting. They are individually divergent for a given fermion due to the ABJ anomaly (21). Those divergencies cancel when summed over a complete generation of quarks and leptons. However, the low loop momentum region does not fully cancel due to different fermion masses and strong interaction effects. So, one needs to carefully evaluate the light quark contributions in a manner that respects the short-distance quark properties (which are not renormalized by strong interactions) (19) but at the same time preserves (22) the chiral properties of the massless quark limit, $m_u = m_d = 0$. Such an analysis was carried out (19) utilizing the Operator Product Expansion. Its detailed numerical results are included in Eq. (17). It was observed in that study that a constituent quark mass calculation (15) with $m_u = m_d = 300$ MeV and $m_s = 500$ MeV combined with the pion pole contribution (22) (avoiding short-distance double counting) reproduces very accurately the results of a much more detailed hadronic model calculation (17). Such an approach is also useful for the light-by-light (LBL) contribution to $a_\mu^{\rm hadronic}$ which is discussed in Section 5.

4 HADRONIC VACUUM POLARIZATION AT LOWEST ORDER

4.1 Outline of the calculation

Unlike the QED part, the contribution from hadronic polarization in the photon propagator (Fig. 4) cannot currently be computed from theory alone, because most of the contributing hadronic physics occurs in the low-energy nonperturbative QCD regime. However, by virtue of the analyticity of the vacuum polarization correlator, the contribution of the hadronic vacuum polarization to a_μ can

be calculated via the dispersion integral (23)

$$a_\mu^{\rm had,LO} \;=\; \frac{\alpha^2(0)}{3\pi^2}\int\limits_{4m_\pi^2}^{\infty} ds\,\frac{K(s)}{s}R(s)\;, \tag{19}$$

where $K(s)$ is the QED kernel (24) ,

$$K(s) = x^2\left(1-\frac{x^2}{2}\right) + (1+x)^2\left(1+\frac{1}{x^2}\right)\left(ln(1+x) - x + \frac{x^2}{2}\right) + \frac{(1+x)}{(1-x)}x^2\,lnx\,, \tag{20}$$

with $x = (1-\beta_\mu)/(1+\beta_\mu)$ and $\beta_\mu = (1-4m_\mu^2/s)^{1/2}$. In Eq. (19), $R(s) \equiv R^{(0)}(s)$ denotes the ratio of the 'bare' cross section for e^+e^- annihilation into hadrons to the lowest-order muon-pair cross section. The 'bare' cross section is defined as the measured cross section, corrected for initial state radiation, electron-vertex loop contributions and vacuum polarization effects in the photon propagator. The reason for using the 'bare' (*i.e.* lowest order) cross section is that a full treatment of higher orders is anyhow needed at the level of a_μ, so that the use of 'dressed' cross sections would entail the risk of double-counting some of the higher-order contributions, or in some cases may actually incorrectly evaluate some of the higher order contributions.

The function $K(s)$ decreases monotonically with increasing s. It gives a strong weight to the low energy part of the integral in Eq. (19). About 91% of the total contribution to $a_\mu^{\rm had,LO}$ is accumulated at center-of-mass energies $\sqrt{s}$ below 1.8 GeV and 73% of $a_\mu^{\rm had,LO}$ is covered by the two-pion final state which is dominated by the $\rho(770)$ resonance.

Many calculations of the hadronic vacuum polarization contribution have been carried out in the past taking advantage of the e^+e^- data available at that time. Clearly, the results depend crucially on the quality of the input data which has been improving in time with better detectors and higher luminosity machines.

Therefore the later calculations, with more complete and better quality data, supersede the results of the former ones. In addition, some approaches make use of theory constraints not only in the high energy region where perturbative QCD applies (25–27), but also at lower energy (28, 29). Also, it was proposed (30) to use data on hadronic τ decays to extract the relevant spectral functions, indeed more precisely known than the e^+e^--based results available then.

In this review, we will follow the latest published analysis by Davier-Eidelman-Höcker-Zhang (DEHZ) (31), which considers both e^+e^- and τ input. Comparison with other independent approaches will later be presented.

4.2 The input data from e^+e^- annihilation

4.2.1 THE MEASUREMENTS The exclusive low-energy e^+e^- cross sections have been mainly measured by experiments running at e^+e^- colliders in Novosibirsk and Orsay. Due to the higher hadron multiplicity at energies above $\sim$ 2.5 GeV, the exclusive measurement of the many hadronic final states is not practicable. Consequently, the experiments at the high-energy colliders ADONE, SPEAR, DORIS, PETRA, PEP, VEPP-4, CESR and BEPC have measured the total inclusive cross section ratio R. Complete references to published data are given in Ref. (32).

The most precise $e^+e^- \to \pi^+\pi^-$ measurements come from CMD-2 which are now available in their final form (33), after a significant revision where problems relating to radiative corrections have been corrected. The results are corrected for leptonic and hadronic vacuum polarization, and for photon radiation by the pions (final state radiation – FSR), so that the measured final state corresponds to $\pi^+\pi^-$ including pion-radiated photons and virtual final state QED effects. The

overall systematic error of the final data is quoted to be 0.6% and is dominated by the uncertainties in the radiative corrections (0.4%).

The comparison between the cross section results from CMD-2 and from previous experiments (corrected for vacuum polarization and FSR, according to the procedure discussed in Section 4.2.2) shows agreement within the much larger uncertainties (2-10%) quoted by the older experiments. But the new CMD-2 results only cover the energy range from 0.61 to 0.96 GeV, so the older data must still be relied upon below and above these values.

Among other exclusive channels with important contributions the process $e^+e^- \to \pi^+\pi^-\pi^0\pi^0$ shows rather large discrepancies among different experiments. In some cases measurements are incomplete, as for example $e^+e^- \to K\overline{K}\pi\pi$ or $e^+e^- \to 6\pi$, and one has to rely on isospin symmetry to estimate or bound the unmeasured cross sections.

4.2.2 RADIATIVE CORRECTIONS TO e^+e^- DATA The evaluation of the integral in Eq. (19) requires the use of the 'bare' hadronic cross section, so that the input data must be analyzed with care in this respect. Several steps are to be considered in the radiative correction procedure:

- The hadronic cross sections given by the experiments are always corrected for initial state radiation and the effect of loops at the electron vertex.
- The vacuum polarization correction in the photon propagator is a more delicate point. The cross sections need to be corrected, *i.e.*

$$\sigma_{\rm bare} = \sigma_{\rm dressed} \left(\frac{\alpha(0)}{\alpha(s)}\right)^2 , \tag{21}$$

  where $\sigma_{\rm dressed}$ is the measured cross section already corrected for initial state radiation, and $\alpha(s)$ takes into account leptonic and hadronic vacuum

polarization. The new data from CMD-2 (33) are explicitly corrected for both leptonic and hadronic vacuum polarization effects (the latter involving an iterative procedure), whereas data from older experiments in general were not.

In fact, what really matters is the correction to the ratio of the hadronic cross section to the cross section for the process used for the luminosity determination. Generally the normalization is done with respect to large angle Bhabha scattering events. In the $\pi^+\pi^-$ mode, all experiments before the latest CMD-2 results corrected their measured processes ($\pi^+\pi^-$, $\mu^+\mu^-$ and e^+e^-) for radiative effects using $O(\alpha^3)$ calculations which took only leptonic vacuum polarization into account (34, 35). For those older experiments, a correction $C_{\rm HVP}$ is applied for the missing hadronic vacuum polarization given by (36)

$$C_{\rm HVP} = \frac{1-2\Delta\alpha_{\rm had}(s)}{1-2\Delta\alpha_{\rm had}(\overline{t})} , \tag{22}$$

where the correction in the denominator applies to the Bhabha cross section evaluated at a mean value of the squared momentum transfer t, which depends on the angular acceptance in each experiment. A 50% uncertainty is assigned to $C_{\rm HVP}$.

- In Eq. (19) $R(s)$ must include the contribution of all hadronic states produced at the energy $\sqrt{s}$, in particular those with FSR. Investigating the existing data in this respect is also a difficult task. In the $\pi^+\pi^-$ data from CMD-2 (33) most additional photons are experimentally rejected to reduce backgrounds from other channels and the fraction kept is subtracted using the Monte Carlo simulation which includes a model for FSR. Then the full FSR contribution is added back as a correction, $C_{\rm FSR}$, using an analytical

expression computed using scalar QED (point-like pions) (37). As this effect was not included in earlier analyses, the same correction is applied to older $\pi^+\pi^-$ data and assigned a 100% uncertainty.

The different corrections in the $\pi^+\pi^-$ contribution amount to -2.3% for leptonic vacuum polarization, $+0.9\%$ for hadronic vacuum polarization, and $+0.9\%$ for FSR. The correction $C_{\rm HVP}$ is small, typically 0.56%.

4.3 The input data from τ decays

4.3.1 Spectral functions from τ decays Data from τ decays into two- and four-pion final states $\tau^- \to \nu_\tau \pi^- \pi^0$, $\tau^- \to \nu_\tau \pi^- 3\pi^0$ and $\tau^- \to \nu_\tau 2\pi^- \pi^+ \pi^0$, are available from ALEPH (38), CLEO (39, 40) and OPAL (41). Recently, preliminary results on the full LEP1 statistics have been presented by ALEPH (42).

Assuming (for the moment) isospin invariance to hold, the corresponding e^+e^- isovector cross sections are calculated via the Conserved Vector Current (CVC) relations

$$\sigma^{I=1}_{e^+e^-\to\pi^+\pi^-} = \frac{4\pi\alpha^2}{s}\, v_{\pi^-\pi^0}\ , \tag{23}$$

$$\sigma^{I=1}_{e^+e^-\to\pi^+\pi^-\pi^+\pi^-} = 2\cdot\frac{4\pi\alpha^2}{s}\, v_{\pi^- 3\pi^0}\ , \tag{24}$$

$$\sigma^{I=1}_{e^+e^-\to\pi^+\pi^-\pi^0\pi^0} = \frac{4\pi\alpha^2}{s}\, [v_{2\pi^-\pi^+\pi^0} - v_{\pi^- 3\pi^0}]\ . \tag{25}$$

The τ spectral function $v_V(s)$ for a given vector hadronic state V is defined by (43)

$$v_V(s) \equiv \frac{m_\tau^2}{6\,|V_{ud}|^2\, S_{\rm EW}}\, \frac{B(\tau^-\to\nu_\tau\, V^-)}{B(\tau^-\to\nu_\tau\, e^-\,\bar\nu_e)}\, \frac{dN_V}{N_V\, ds}\, \left[\left(1-\frac{s}{m_\tau^2}\right)^2\, \left(1+\frac{2s}{m_\tau^2}\right)\right]^{-1}, \tag{26}$$

where $|V_{ud}| = 0.9748 \pm 0.0010$ is obtained from averaging the determinations (44)

from nuclear β decays and kaon decays (assuming unitarity of the CKM matrix) and $S_{\rm EW}$ accounts for electroweak radiative corrections as discussed in Section 4.3.2. The spectral functions are obtained from the corresponding invariant mass distributions, subtracting out the non-τ background and the feedthrough from other τ decay channels, and after a final unfolding from detector response. Note that the measured τ spectral functions are inclusive with respect to radiative photons.

It should be pointed out that the experimental conditions at the Z pole (ALEPH, OPAL) and at the $\Upsilon(4S)$ (CLEO) energies are very different. On the one hand, at LEP, the $\tau^+\tau^-$ events can be selected with high efficiency ($> 90\%$) and small non-τ background ($< 1\%$), thus ensuring little bias in the efficiency determination. Despite higher background and smaller efficiency, CLEO has the advantage of lower energy for the reconstruction of the decay final state since particles are more separated in space. One can therefore consider ALEPH/OPAL and CLEO data to be approximately uncorrelated as far as experimental procedures are concerned. The fact that their respective spectral functions for the $\pi^-\pi^0$ and $2\pi^-\pi^+\pi^0$ modes agree is therefore a valuable experimental consistency test.

4.3.2 Isospin symmetry breaking The relationships (23), (24) and (25) between e^+e^- and τ spectral functions only hold in the limit of exact isospin invariance. It follows from the factorization of strong interaction physics as produced through the γ and W propagators out of the QCD vacuum. However, symmetry breaking is expected at some level from electromagnetic processes, whereas the small u,d mass splitting leads to negligible effects. Various identified sources of isospin breaking are considered in the dominant 2π channel.

- Electroweak radiative corrections yield their dominant contribution from the short distance correction to the effective four-fermion coupling $\tau^- \to \nu_\tau (d\bar{u})^-$ enhancing the τ amplitude by the factor $(1 + 3\alpha(m_\tau)/4\pi)(1 + 2\overline{Q}) \ln(M_Z/m_\tau)$, where $\overline{Q}$ is the average charge of the final state partons (45, 46). While this correction vanishes for leptonic decays, it contributes for quarks. All higher-order logarithms can be resummed using the renormalization group (45,47) into an overall multiplicative electroweak factor $S_{\rm EW}^{\rm had}$, which is equal to 1.0194. The difference between the resummed value and the lowest-order estimate (1.0188) can be taken as a conservative estimate of the uncertainty. QCD corrections to $S_{\rm EW}^{\rm had}$ have been calculated (45, 46) and found to be small, reducing its value to 1.0189. Subleading non-logarithmic short distance corrections have been calculated to order $O(\alpha)$ for the leptonic width (45), $S_{\rm EW}^{\rm sub,lep} = 1 + \alpha(25/4 - \pi^2)/2\pi \simeq 0.9957$.

- A contribution (30, 48) for isospin breaking occurs because of the mass difference between charged and neutral pions, which is essentially of electromagnetic origin. The spectral function has a kinematic factor β^3 which is different in e^+e^- $(\pi^+\pi^-)$ and τ decay $(\pi^-\pi^0)$,

$$v_{0,-}(s) = \frac{\beta_{0,-}^3(s)}{12} |F_\pi^{0,-}(s)|^2 \ , \tag{27}$$

  $F_\pi^{0,-}(s)$ being the electromagnetic and weak pion form factors, respectively, where $\beta_{0,-} = \beta(s, m_{\pi^-}, m_{\pi^{+,0}})$ is given in (32).

- Other corrections occur in the form factor itself. It is affected by the pion mass difference because the same β^3 factor enters in the $\rho \to \pi\pi$ width. This effect partially compensates the β^3 correction (27) of the cross section. Similarly, mass and width differences between the charged and neutral ρ

meson (30, 49, 50) will affect the resonance lineshape. Such effects can be investigated directly on the measured spectral functions.

- $\rho - \omega$ interference occurs in the $\pi^+\pi^-$ mode only, but its contribution can be readily introduced into the τ spectral function using the parameters determined in the CMD-2 fit (33). Also, electromagnetic decays explicitly break SU(2) symmetry for the ρ width. This is the case for the decays $\rho \to \pi\pi^0\gamma$, $\pi\gamma$ and $\rho^0 \to \eta\gamma$, l^+l^-. Calculations have been done for the decay $\rho \to \pi\pi\gamma$ with an effective model (51).

- Long distance corrections are expected to be final-state dependent in general. A consistent calculation of radiative corrections for the $\nu_\tau\pi^-\pi^0$ mode has been recently performed including the effect of loops (52, 53). The τ spectral function must be divided by a factor $S_{\rm EW}^{\pi\pi^0}(s)$,

$$S_{\rm EW}^{\pi\pi^0}(s) = \frac{S_{\rm EW}^{\rm had} G_{\rm EM}(s)}{S_{\rm EW}^{\rm sub,lep}} = (1.0233 \pm 0.0006) \cdot G_{\rm EM}(s) \ , \qquad (28)$$

where $G_{\rm EM}(s)$ is the long-distance radiative correction involving both real photon emission and virtual loops. The form factor correction is dominated by the effect of the pion mass difference in the ρ width, so that the correction is rather independent from the chosen parametrization of the form factor.

Finally, the total correction to $a_\mu^{\rm hadronic}$ from isospin-breaking using the τ 2π data amounts to $(-9.3 \pm 2.4)\ 10^{-10}$.

4.4 Confronting e^+e^- and τ data

The new e^+e^- and the isospin-breaking corrected τ spectral functions can be directly compared for the $\pi\pi$ final state. The τ spectral function is obtained by averaging ALEPH (38), CLEO (39) and OPAL (41) results (32). The e^+e^- data

are plotted as a point-by-point ratio to the τ spectral function in Fig. 5. The central bands in Fig. 5 give the quadratic sum of the statistical and systematic errors of the τ spectral function obtained by combining all τ data. The e^+e^- and τ data are consistent below and around the ρ peak, while a discrepancy persists for energies larger than 0.85 GeV. Part of the discrepancy could originate from different masses and widths for the neutral and charged ρ's, but correcting for this effect has the result of spreading the disagreement over a wider mass range (49, 57).

A convenient way to assess the compatibility between e^+e^- and τ spectral functions proceeds with the evaluation of the τ decay fractions using the relevant e^+e^- spectral functions as input. This procedure provides a quantitative comparison using a single number. Employing the branching fraction $B(\tau^- \to \nu_\tau\, e^-\, \bar{\nu}_e) = (17.810 \pm 0.039)\%$, obtained assuming leptonic universality in the charged weak current (42), the predicted branching ratio is

$$\mathcal{B}_{\rm CVC}(\tau^- \to \nu_\tau \pi^- \pi^0) = (24.52 \pm 0.26_{\rm exp} \pm 0.11_{\rm rad} \pm 0.12_{\rm SU(2)})\ \%\ , \qquad (29)$$

where the errors quoted are split into uncertainties from the experimental input (the e^+e^- annihilation cross sections) and the numerical integration procedure, the missing radiative corrections applied to the relevant e^+e^- data, and the isospin-breaking corrections when relating τ and e^+e^- spectral functions. The result in Eq. (29) disagrees with the direct measurement,

$$\mathcal{B}_{\rm exp}(\tau^- \to \nu_\tau \pi^- \pi^0) = (25.46 \pm 0.10)\ \%\ . \qquad (30)$$

Even though the revision in the CMD-2 results have reduced the discrepancy between Eq. (29) and the measurement from 4.6 to 2.9 standard deviations (adding all errors in quadrature), the remaining difference of $(-0.94 \pm 0.10_\tau \pm 0.26_{\rm ee} \pm$

$0.11_{\rm rad} \pm 0.12_{\rm SU(2)} (\pm 0.32_{\rm total}))\%$ is still problematic. Since the disagreement between e^+e^- and τ spectral functions is more pronounced at energies above 850 MeV, we expect a smaller discrepancy in the calculation of $a_\mu^{\rm had,LO}$ because of the steeply falling function $K(s)$. More information on the comparison is displayed in Fig. 6 where it is clear that ALEPH, CLEO, L3 and OPAL all separately, but with different significance, disagree with the e^+e^--based CVC result.

The discrepancy between e^+e^- and τ spectral functions prevents us from presenting a unique evaluation of the dispersion integral profiting from both sources. On one hand, it is clear that e^+e^- data is the natural input and that τ data need additional treatment to cope with isospin breaking corrections. On the other hand, recent history has taught us that reliability on the input data is an important concern and therefore redundancy is needed. This is achieved within the τ data sets, but not yet with e^+e^- data as it relies on only one precise experiment. The forthcoming results from KLOE (63) and BABAR (64) are very important in that respect to assess the consistency of the e^+e^- input.

4.5 Special cases

4.5.1 The threshold region To overcome the lack of precise data at threshold energies and to benefit from the analyticity property of the pion form factor, a third order expansion in s is used:

$$F_\pi^0 \;=\; 1 + \frac{1}{6}\langle r^2\rangle_\pi \, s + c_1 \, s^2 + c_2 \, s^3 + O(s^4) \; . \tag{31}$$

Exploiting precise results from space-like data (65), the pion charge radius-squared is constrained to $\langle r^2\rangle_\pi = (0.439 \pm 0.008)$ fm^2 and the two parameters $c_{1,2}$ are fitted to the data in the range $[2m_\pi,\ 0.6\ \text{GeV}]$. Good agreement is observed in the low energy region where the expansion should be reliable. Since the fits in-

corporate unquestionable constraints from first principles, this parameterization is used for evaluating the integrals in the range up to 0.5 GeV.

4.5.2 QCD FOR THE HIGH ENERGY CONTRIBUTIONS Since problems still remain regarding the spectral functions from low-energy data, a conservative choice of using the QCD prediction only above an energy of 5 GeV is adopted. The details of the calculation can be found in (26,29) and in the references therein.

The perturbative QCD prediction uses a next-to-next-to-leading order $O(\alpha_s^3)$ expansion of the Adler D-function (66), with second-order quark mass corrections included (67). $R(s)$ is obtained by evaluating numerically a contour integral in the complex s plane. Nonperturbative effects are considered through the Operator Product Expansion, giving power corrections controlled by gluon and quark condensates. The value $\alpha_s(M_Z^2) = 0.1193 \pm 0.0026$, used for the evaluation of the perturbative part, is taken as the average of the results from the analyses of τ decays (68) and of the Z width in the global electroweak fit (69). The two determinations have comparable uncertainties (mostly theoretical for the τ and experimental for the Z) and agree well with each other. Uncertainties are taken to be equal to the common error on $\alpha_s(M_Z^2)$, to half of the quark mass corrections and to the full nonperturbative contributions. A test of the QCD prediction can be performed in the energy range between 1.8 and 3.7 GeV. The contribution to $a_\mu^{\rm had,LO}$ in this region is computed to be $(338.7 \pm 4.6)\ 10^{-11}$ using QCD, to be compared with the result, $(349 \pm 18)\ 10^{-11}$ from the data. The two values agree within the 5% accuracy of the measurements.

In Ref. (29) the evaluation of $a_\mu^{\rm had,LO}$ was shown to be improved by applying QCD sum rules. We do not consider this possibility here for the following two reasons. First, it is clear that the main problem at energies below 2 GeV is now

the inconsistency between the e^+e^- and τ input data, and this must be resolved with priority. Second, the improvement provided by the use of QCD sum rules results from a balance between the experimental accuracy of the data and the theoretical uncertainties. The present precision of both e^+e^- and τ data, should they agree, is such that the gain would be smaller than before.

4.6 Results for the LO hadronic vacuum polarization

Fig. 7 gives a panoramic view of the e^+e^- data in the relevant energy range. The shaded band below 2 GeV represents the sum of the exclusive channels considered in the analysis. The QCD prediction is indicated by the cross-hatched band, used here only for energies above 5 GeV. Note that the QCD band is plotted taking into account the thresholds for open flavour B states, in order to facilitate the comparison with the data in the continuum. However, for the evaluation of the integral, the $b\overline{b}$ threshold is taken at twice the pole mass of the b quark, so that the contribution includes the narrow Υ resonances, according to global quark-hadron duality.

The discrepancies discussed above are now expressed directly in terms of $a_\mu^{\rm had,LO}$, giving smaller estimates for the e^+e^--based data set by $(-119 \pm 73)\ 10^{-11}$ for the $\pi\pi$ channel and $(-28 \pm 29)\ 10^{-11}$ for the sum of the 4π channels. The total difference $(-147 \pm 79)\ 10^{-11}$ could now be considered to be acceptable, however the systematic difference between the e^+e^- and τ $\pi\pi$ spectral functions at high energies precludes one from performing a straightforward combination of the two evaluations.

The results for the lowest order hadronic contribution are

$$\begin{aligned} a_\mu^{\rm had,LO} &= (6963 \pm 62_{\rm exp} \pm 36_{\rm rad})\ 10^{-11} && [\text{DEHZ } e^+e^- \text{based}] \ , \\ a_\mu^{\rm had,LO} &= (7110 \pm 50_{\rm exp} \pm 8_{\rm rad} \pm 28_{\rm SU(2)})\ 10^{-11} && [\text{DEHZ } \tau \text{based}] \ . \end{aligned} \tag{32}$$

4.7 Comparison between different analyses

As pointed out before it only makes sense to compare estimates based on the same input data, considering the fact that previously available CMD-2 data were significantly corrected in their last publication (33). Besides the approach described above using both e^+e^- and τ spectral functions two other determinations are available. The calculation presented by Hagiwara-Martin-Nomura-Teubner (HMNT) (70) also proceeds using the complete set of available exclusive channels up to 1.4 GeV, but only inclusive measurements above. The two main differences between this estimate and the one described is the treatment of data in the threshold region and the use of inclusive data between 1.4 and 2 GeV. In both cases, the results are consistent within the experimental errors, but the analysis (70) yields lower central values with a more agressive theoretical error. It is difficult to comment on the second determination by Ghozzi-Jegerlehner (GJ) (50) as it has been presented without any information about the data used, the way they are handled and the different contributions to the final error. The values found,

$$\begin{aligned} a_\mu^{\rm had,LO} &= (6961.5 \pm 57_{\rm exp} \pm 24_{\rm rad})\ 10^{-11} && [\text{HMNT exclusive (70)}] \ , \\ a_\mu^{\rm had,LO} &= (6948 \pm 86)\ 10^{-11} && [\text{GJ (50)}] \ , \end{aligned} \tag{33}$$

are in agreement with the e^+e^--based results Eq. (32) found in the DEHZ analysis. Though the experimental errors should be strongly correlated, differences

between the analyses could result from the treatment of experimental systematic uncertainties, the numerical integration procedure (averaging or not neighboring data points) and the treatment of missing radiative corrections.

The value given by HMNT using the inclusive e^+e^- data between 1.4 and 2 GeV is consistent within one standard deviation (computed with respect to the respective inclusive-exclusive uncertainties in the 1.4-2 GeV range), but turns out to be somewhat smaller,

$$a_\mu^{\rm had,LO} \;=\; (6924 \pm 59_{\rm exp} \pm 24_{\rm rad})\; 10^{-11} \qquad \text{[HMNT inclusive (70)]}\;. \tag{34}$$

Since the e^+e^- exclusive and inclusive predictions agree within errors, we combine them into a single mean value, using the more conservative error estimate,

$$a_\mu^{\rm had,LO} = (6944 \pm 62_{\rm had,LO} \pm 36_{\rm rad})\; 10^{-11} \quad \text{[e$^+$e$^-$ average]}. \tag{35}$$

5 HADRONIC THREE-LOOP EFFECTS

The three-loop hadronic contributions to $a_\mu^{\rm SM}$ involve one hadronic vacuum polarization insertion with an additional loop (either photonic or another leptonic or hadronic vacuum polarization insertion). They can be evaluated (71) using the same $e^+e^- \to$ hadrons data sets described in Section 4. Calling that subset of $\mathcal{O}(\alpha/\pi)^3$ hadronic contributions $a_\mu^{\rm had,NLO}$, we quote here the result of a recent analysis (70),

$$a_\mu^{\rm had,NLO} = -98(1) \times 10^{-11}\;, \tag{36}$$

which is consistent with earlier studies (30, 71). It would change by about -3×10^{-11} if the τ data described in Section 4 were used.

More controversial are the hadronic light-by-light scattering contributions illustrated in Fig. 8. A dispersion relation approach using data is not possible

and a first-principles calculation (e.g. lattice gauge theory (72)) has not been carried out. Instead, calculations involving pole insertions, short-distance quark loops (73) and charged-pion loops have been individually performed in a large N_c QCD approach. The pseudoscalar poles (π°, η and η') dominate such a calculation. Unfortunately, in early studies the sign of their contribution was incorrect and misleading. Its correction (74) led to a large shift in the $a_\mu^{\rm SM}$ prediction. A representative estimate (32) of the LBL contribution which includes π, η and η' poles as well as other resonances, charged pion loops and quark loops currently gives

$$a_\mu^{\rm had,LBL} \simeq 86(35) \times 10^{-11} \qquad \text{[representative]} \ . \tag{37}$$

Recently, however, a new analysis of LBL was given by Melnikov and Vainshtein (MV) (75). Their approach for the first time properly matches the asymptotic short-distance behavior of pseudoscalar and axial-vector contributions with the free quark loop behavior. It yields the somewhat larger result,

$$a_\mu^{\rm had,LBL} = 136(25) \times 10^{-11} \qquad \text{[MV (75)]} \ . \tag{38}$$

We note, however, that several small but (likely) negative contributions such as charged pion loops and scalar resonances were not included and could reduce the magnitude of the result in Eq.(38), but probably not too significantly. In fact, MV provide a consistency check on their result much in the spirit of the EW hadronic triangle diagram study (19, 76) discussed in Section 3. Using constituent quark masses in the light-by-light diagram combined with a pion pole contribution that properly accounts for the chiral properties of massless QED and avoiding short-distance double counting, the authors find $a_\mu^{\rm had,LBL} \simeq 120 \times 10^{-11}$ with about half of the contribution coming from quark diagrams and the other half from the pion pole. We employ that result along with a rather conservative error assigned

by us so that the results in Eqs. (37) and (38) overlap within their errors,

$$a_\mu^{\rm had,LBL} \simeq 120(35) \times 10^{-11} \ . \tag{39}$$

Further resolution of the LBL contribution is very important. At present, we employ the result in Eq. (39) for comparison with experiment. In that way, one finds from Eqs. (36) and (39)

$$a_\mu^{\rm had,3-loop} = 22(35) \times 10^{-11} \ . \tag{40}$$

That value is reduced by about 3×10^{-11} if τ data are used.

6 COMPARISON OF THEORY AND EXPERIMENT

Collecting the results from previous sections on $a_\mu^{\rm QED}$, $a_\mu^{\rm EW}$, $a_\mu^{\rm had,LO}$, $a_\mu^{\rm had,NLO}$, and $a_\mu^{\rm had,LBL}$, the Standard Model prediction for a_μ can be obtained. Since the situation on $a_\mu^{\rm had,LO}$ is not yet settled, it is unavoidable to quote two values using the e^+e^- (31, 50, 70) and the τ decay data (31),

$$\begin{aligned} a_\mu^{\rm SM} &= (116\,591\,841 \pm 72_{\rm had,LO} \pm 35_{\rm LBL} \pm 3_{\rm QED+EW})\ 10^{-11} \qquad [e^+e^-] \ , \\ a_\mu^{\rm SM} &= (116\,592\,004 \pm 58_{\rm had,LO} \pm 35_{\rm LBL} \pm 3_{\rm QED+EW})\ 10^{-11} \qquad [\tau] \ . \end{aligned} \tag{41}$$

The SM values can be compared to the measurement (13). Keeping experimental and theoretical errors separate, the differences between measured and predicted values, $\Delta a_\mu = a_\mu^{\rm exp} - a_\mu^{\rm SM}$, are found to be

$$\begin{aligned} \Delta a_\mu &= (239 \pm 72_{\rm had,LO} \pm 35_{\rm other} \pm 58_{\rm exp})\ 10^{-11} \qquad [e^+e^-] \ , \\ \Delta a_\mu &= (\ 76 \pm 58_{\rm had,LO} \pm 35_{\rm other} \pm 58_{\rm exp})\ 10^{-11} \qquad [\tau] \ , \end{aligned} \tag{42}$$

where the first error quoted is specific to each approach, the second is due to contributions other than hadronic vacuum polarization, and the third is the BNL

g-2 experimental error. The last two errors are identical in both evaluations. Adding all errors in quadrature, the differences in Eq. (42) correspond to 2.4 and 0.9 standard deviations, respectively. A graphical comparison of the results with the experimental value is given in Fig. 9. A word of caution is in order about the real meaning of "standard deviations" as the uncertainty in the theoretical prediction is dominated by systematic errors in the e^+e^- experiments for which a gaussian distribution is questionable.

At this point we repeat that the e^+e^--based estimate is the most direct one and should be in general prefered. However, since the e^+e^--τ discrepancy is still unresolved and the e^+e^- results rely on only one precise experiment, we find it appropriate to keep in mind the τ-based estimate.

The apparent deviation from the e^+e^--based prediction is of great interest, even if it is not an overwhelming discrepancy. Ordinarily, one would not necessarily worry about a 2.4 σ effect. In fact, the proper response would be to improve the experimental measurement (which is statistics limited) by further running and to continue to improve theory. With regard to the latter, new $e^+e^- \to$ hadrons data and further study of LBL could potentially reduce the overall theoretical uncertainty. The excitement caused by the deviation stems from the expectation that "new physics" could cause a deviation of the magnitude observed in Eq. (42). In the next section, we briefly review several examples.

7 NEW PHYSICS CONTRIBUTIONS

A deviation of about $\sim 240 \times 10^{-11}$ in $\Delta a_\mu = a_\mu^{\rm exp} - a_\mu^{\rm SM}$ would have interesting interpretations if truly due to "new physics". The leading contender for causing such an effect is supersymmetry. Indeed, supersymmetric contributions to a_μ can

stem from sneutrino-chargino and smuon-neutralino loops as illustrated in Fig. 10. Those diagrams actually describe 2-chargino and 4-neutralino states and could include 3-generation slepton mixing. In general, a broad range of predictions are possible depending on particle masses, couplings etc. For illustration purposes, we assume degenerate masses $\sim m_{\rm SUSY}$ in all loops (77) (not a realistic assumption but one that should roughly approximate expectations). Then in terms of $\tan\beta = <\phi_2> / <\phi_1>$, the ratio of Higgs vacuum expectations and sgn $\mu = \pm$, one finds (for $\tan\beta \geq 3$) $a_\mu^{\rm SUSY} \simeq ({\rm sgn}\mu) \times 130 \times 10^{-11}$ (100 GeV/$m_{\rm SUSY}$)^2 $\tan\beta$ where 2-loop leading-log QED suppression effects have been included (12). Equating that prediction with a $+240 \times 10^{-11}$ deviation suggests sgn $\mu = +$ and $m_{\rm SUSY} \simeq 74\sqrt{\tan\beta}$ GeV.

The sgn $\mu = +$ scenario is also favored by $b \to s\gamma$ data while for $3 \leq \tan\beta \leq 40$ the range 127 GeV $\leq m_{\rm SUSY} \leq$ 465 GeV is in keeping with expectations of SUSY enthusiasts. So, a deviation in Δa_μ of about the apparent magnitude is a relatively generic prediction of low mass SUSY models. If SUSY is eventually discovered at high-energy colliders and the masses measured, one can use Δa_μ to determine $\tan\beta$.

Another generic possibility (78) is "new physics" related to the origin of the muon mass via loop effects (radiative muon mass scenarios). In such schemes (12) the muon mass originates from a chiral symmetry breaking loop effect with its origin coming from a high scale M which can arise from dynamics, extra dimensions, multi-Higgs, softly broken SUSY, etc. One finds generically $a_\mu(M) \simeq C(m_\mu^2/M^2)$ where C is $\mathcal{O}(1)$ rather than (α/π). A deviation of $\Delta a_\mu \simeq 240 \times 10^{-11}$ corresponds to $M \simeq 2$ TeV, an interesting possibility. Indeed, if SUSY is not found at high energy colliders, it is highly likely that other $\mathcal{O}(1$ TeV) scale physics

emerges. If the Δa_μ deviation is related, it would suggest that mass generating "new physics" is at hand.

Other forms of "new physics" (12) such as Z' or W_R bosons, anomalous W dipole moments etc. generally lead to unobservely small Δa_μ. So, SUSY with its relatively low mass scale and tan β enhancement along with models with no α/π suppression are the more natural candidates to explain a deviation in Δa_μ from zero.

8 OUTLOOK

After considerable effort, the experiment E821 at Brookhaven has improved the determination of a_μ by about a factor of 14 relative to the classic CERN results of the 1970's (79). The result is still statistics-limited and could be improved by another factor of 2 or so (to a precision of 30×10^{-11}) before systematics effects become a limitation. Pushing the experiment to that level seems to be an obvious goal for the near term. In the longer term, a new experiment with improved muon acceptance and magnetic fields could potentially reach 6×10^{-11} (80).

The theoretical prediction within the Standard Model is more of a limitation. The current 80×10^{-11} error is dominated by uncertainties in $e^+e^- \to$ hadrons which lead to about a 1% error in the evaluation of the hadronic vacuum polarization contribution. This estimate relies so far primarily on only one precise experiment, so that it is very desirable to secure redundancy. Data obtained with a different technique, such as the radiative return process $e^+e^- \to \gamma +$ hadrons (63, 64), will provide a nice consistency check and could lead to a reduction of the error. Progress is also needed in the development of cross-checked Monte Carlo programs to apply radiative corrections with an increased con-

fidence. The consideration of the τ data, which currently disagrees with the available e^+e^- results, should be reviewed after consolidation of the e^+e^- data, revisiting the isospin-breaking corrections. Finally, lattice gauge theories with dynamical fermions (72) can in principle provide a determination of $a_\mu^{\rm had,LO}$. All sources considered, and assuming all discrepancies to be resolved, it appears difficult to reach an uncertainty much better than 35×10^{-11} in this sector.

The 30% uncertainty in hadronic LBL contributions (35×10^{-11}) is largely model-dependent. Here one could imagine that further work following the MV approach (75) or a lattice calculation could reduce the error by a factor of 2. Doing much better appears to be difficult, but such an improvement would be well matched to short-term experimental capabilities.

If the above experimental and theoretical improvements do occur, they will lead to a total uncertainty in $\Delta a_\mu = a_\mu^{\rm exp} - a_\mu^{\rm SM}$ of about 50×10^{-11}, *i.e.* a factor of 2 reduction. This would provide a very important step in testing the SM, particularly if the current difference persists, as it would translate to a $\sim 5\ \sigma$ discrepancy. The result could be used in conjunction with future collider discoveries to sort out the properties of new physics (*e.g.* the size of $\tan\beta$ in SUSY) or constrain further possible appendages to the SM.

Acknowledgements

We wish to thank the many colleagues who contributed to this exciting field.

Literature Cited

1. Dirac PAM, *Proc. Roy. Soc.* **A117** (1928) 610.
2. Schwinger J, *Phys. Rev.* **73** (1948) 416L.

3. Nagle J, Nelson E, Rabi I, *Phys. Rev* **71** (1947) 914; Nagle J, Julian R, Zacharias J, *Phys. Rev.* **72** (1947) 971.
4. van Dyck RS, Schwinberg PB, Dehmelt HG, *Phys. Rev. Lett.* **59** (1987) 26.
5. Kinoshita T, Nio M, *Phys. Rev. Lett.* **90** (2003) 021803.
6. Laporta S,and Remiddi E, *Phys. Lett.* **B379** (1996) 283.
7. Czarnecki A, Marciano W, *Nucl. Phys. B Proc.* **76** (1999) 245.
8. Marciano W, in *Proceedings of the Dirac Centennial Symposium*, FSU (2002).
9. Mohr P, Taylor B, *Rev. Mod. Phys.* **72** (2000) 351.
10. Gabrielse G, Tan J, in *Cavity Quantum Electrodynamics*, Ed. Berman P, Academic Press, San Diego (1994) p267.
11. Kinoshita T, in *The Gregory Breit Centennial Symposium*, Eds. Hughes V, Iachello F, Kusnizov D.
12. Czarnecki A, Marciano W, *Phys. Rev* **D64** (2001) 013014.
13. Bennett GW *et al.*, E821 g-2 Collaboration, *Phys. Rev Lett.* **89** (2002)101804; hep-ex/0401008.
14. Kinoshita T (private communication) to be published.
15. Czarnecki A, Krause B, Marciano W, *Phys. Rev.* **D52** (1995) 2619; *Phys. Rev. Lett.* **76** (1996) 3267.
16. Kinoshita T, Nizic B, Okamoto Y, *Phys. Rev.* **D41** (1990) 593; Milstein AI, Yelkhovsky AS, *Phys. Lett.* **B233** (1989) 11; Karshenboim SG, *Phys. Atom. Nucl.* **56** (1993) 857; Kataev AL, Starshenko VV, *Phys. Rev.* **D52** (1995) 402.
17. Jackiw R, Weinberg S, *Phys. Rev.* **D5** (1972) 2396; Altarelli G, Cabibbo N, Maiani L, *Phys. Lett.* **B40** (1972) 415; Bars I, Yoshimura M, *Phys. Rev.* **D6** (1972) 374; Fujikawa K, Lee BW, Sanda AI, *Phys. Rev.* **D6** (1972) 2923.

18. Kukhto T, Kuraev EA, Schiller A, Silagadze ZK, *Nucl. Phys.* **B371** (1992) 567.

19. Czarnecki A, Marciano W, Vainshtein A, *Phys. Rev.* **D67** (2003) 073006.

20. Degrassi G, Giudice GF, *Phys. Rev.* **D58** (1998) 053007.

21. Adler SL, *Phys. Rev.* **177** (1969) 2426; Bell J, Jackiw R, *Nuovo Cim.* **A60** (1969) 47.

22. Peris S, Perrottet M, de Rafael E, *Phys. Lett.* **B355** (1995) 523; Knecht M *et al.*, *JHEP***0211** (2002) 003.

23. Gourdin M, de Rafael E, *Nucl. Phys.* **B10** (1969) 667.

24. Brodsky SJ, de Rafael E, *Phys. Rev.* **168** (1968) 1620.

25. Martin AD, Zeppenfeld D, *Phys. Lett.* **B345** (1995) 558.

26. Davier M, Höcker A, *Phys. Lett.* **B419** (1998) 419.

27. Kühn JH, Steinhauser M, *Phys. Lett.* **B437** (1998) 425.

28. Groote S *et al.*, *Phys. Lett.* **B440** (1998) 375.

29. Davier M, Höcker A, *Phys. Lett.* **B435** (1998) 427.

30. Alemany R, Davier M, Höcker A, *Eur.Phys.J.* **C2** (1998) 123.

31. Davier M, Eidelman S, Höcker A, Zhang Z, *Eur.Phys.J.* **C31** (2003) 503.

32. Davier M, Eidelman S, Höcker A, Zhang Z, *Eur.Phys.J.* **C27** (2003) 497.

33. Akhmetshin R *et al.* (CMD-2 Collaboration), hep-ex/0308008.

34. Bonneau G, Martin F, *Nucl. Phys.* **B27** (1971) 381.

35. Eidelman S, Kuraev E, *Phys. Lett.* **B80** (1978) 94.

36. Swartz ML, *Phys. Rev.* **D53** (1996) 5268.

37. Höfer A, Gluza J, Jegerlehner F, *Eur. Phys. J.* **C24** (2002) 51.

38. Barate R *et al.*, (ALEPH Collaboration), *Z. Phys.* **C76** (1997) 15.

39. Anderson S *et al.* (CLEO Collaboration), *Phys.Rev.* **D61** (2000) 112002.

40. Edwards KW *et al.* (CLEO Collaboration), *Phys.Rev.* **D61** (2000) 072003.

41. Ackerstaff K *et al.* (OPAL Collaboration), *Eur. Phys. J.* **C7** (1999) 571.

42. ALEPH Collaboration, ALEPH 2002-030 CONF 2002-019, (July 2002).

43. Tsai P, *Phys. Rev.* **D4** (1971) 2821.

44. Review of Particle Physics, Hagiwara K *et al.*, *Phys. Rev.* **D66** (2002) 010001.

45. Marciano WJ, Sirlin A, *Phys. Rev. Lett.* **61** (1988) 1815.

46. Sirlin A, *Nucl. Phys.* **B196** (1982) 83.

47. Braaten E, Narison S, Pich A, *Nucl. Phys.* **B373** (1992) 581.

48. Czyż H, Kühn JH, *Eur.Phys.J.* **C18** (2001) 497.

49. Davier M, *Spectral functions from hadronic τ decays*, Workshop on e^+e^- Hadronic Cross Section, Pisa, 8-10 October 2003, hep-ex/0312064.

50. Ghozzi S, Jegerlehner F, hep-ph/0310181.

51. Singer P, *Phys. Rev.* **130** (1963) 2441; Erratum-ibid. **161** (1967) 1694.

52. Cirigliano V, Ecker G, Neufeld H, *Phys. Lett.* **B513** (2001) 361.

53. Cirigliano V,Ecker G, Neufeld H, *JHEP* **0208** (2002) 002.

54. Barkov LM *et al.* (OLYA, CMD Coll.), *Nucl. Phys.* **B256** (1985) 365.

55. Vasserman IB *et al.* (OLYA Coll.), *Sov. J. Nucl. Phys.* **30** (1979) 519.

56. Quenzer A *et al.* (DM1 Collaboration), *Phys. Lett.* **B76** (1978) 512.

57. Davier M, *Updated estimate of the muon magnetic moment using revised results from e^+e^- annihilation*, Workshop on e^+e^- Hadronic Cross Section, Pisa, 8-10 October 2003, hep-ex/0312065.

58. Artuso M *et al.* (CLEO Collaboration), *Phys. Rev. Lett.* **72** (1994) 3762.

59. Achard P *et al.* (L3 Collaboration), CERN-EP/2003-019, May 2003,

60. Ackerstaff K *et al.* (OPAL Collaboration), *Eur. Phys. J.* **C4** (1998) 93.

61. Barate R *et al.* (ALEPH Collaboration), *Eur. Phys. J.* **C11** (1999) 599.

62. Battle M *et al.* (CLEO Collaboration), *Phys. Rev. Lett.* **73** (1994) 1079.

63. Valeriani B, *Preliminary results from KLOE on the radiative return*, Workshop on e^+e^- Hadronic Cross Section, Pisa, 8-10 October 2003.

64. Davier M, *Status of the BaBar R measurement using radiative return*, Workshop on e^+e^- Hadronic Cross Section, Pisa, 8-10 October 2003, hep-ex/0312093.

65. Amendolia SR *et al.* (NA7 Collaboration), *Nucl. Phys.* **B277** (1986) 168.

66. Surguladze LR, Samuel MA, *Phys. Rev. Lett.* **66** (1991) 560;
Gorishny SG, Kataev KL, Larin SA, *Phys. Lett.* **B259** (1991) 144.

67. Chetyrkin KG, Kühn JH, Steinhauser M, *Nucl. Phys.* **B482** (1996) 213.

68. Barate R *et al.*, (ALEPH Collaboration), *Eur. J. Phys.* **C4** (1998) 409.

69. LEP Electroweak Working Group, LEPEWWG/2002-01 (May 2002).

70. Hagiwara K, Martin AD, Nomura D, Teubner T, hep-ph/0312250.

71. Krause B, *Phys. Lett.* **B390** (1997) 392.

72. Blum T, *Phys. Rev. Lett.* **91** (2003) 052001.

73. Hayakawa M, Kinoshita T, *Phys. Rev.* **D57** (1998) 465; Bijnens J, Pallante E, Prades J, *Nucl. Phys.* **B474** (1996) 379.

74. Knecht M, Nyffeler A, *Phys. Rev.* **D65** (2002) 073034; Knecht M *et al.*, *Phys. Rev. Lett.* **88** (2002) 071802; Blokland I, Czarnecki A, Melnikov K, *Phys. Rev. Lett.* **88** (2002) 071803; Hayakawa M, Kinoshita K, *Phys. Rev.* **D66** (2002) 019902(E); Bijnens J, Pallante E, Prades J, *Nucl. Phys.* **B626** (2002) 410.

75. Melnikov K, Vainshtein A, hep-ph/0312226.

76. Vainshtein A, *Phys. Lett.* **B569** (2003) 187.

77. Moroi T, *Phys. Rev.* **D53** (1996) 6565; Erratum **D56** (1997) 4424; Ibrahim T, Nath P, *Phys. Rev.* **D57** (1998) 478; Kosower D, Krauss L, Sakai N, *Phys.*

Lett. **B133** (1983) 305.

78. Marciano W, in *Particle Theory and Phenomenology*, Eds. Lassila K *et al.*, World Scientific (1996) p22; *Radiative Corrections Status and Outlook*, Ed. Ward BFL, World Scientific (1995) p403.
79. Bailey J, *et al.*, *Phys. Lett.* **B68** (1977) 191; Farley FJM, Picasso E, *The muon (g-2) Experiments*, Advanced Series on Directions in High Energy Physics - Vol. 7 Quantum Electrodynamics, Ed. Kinoshita T, World Scientific (1990).
80. Roberts BL, in *High Intensity Muon Sources*, Eds. Kuno Y, Yokoi T, World Scientific (1999) p69.

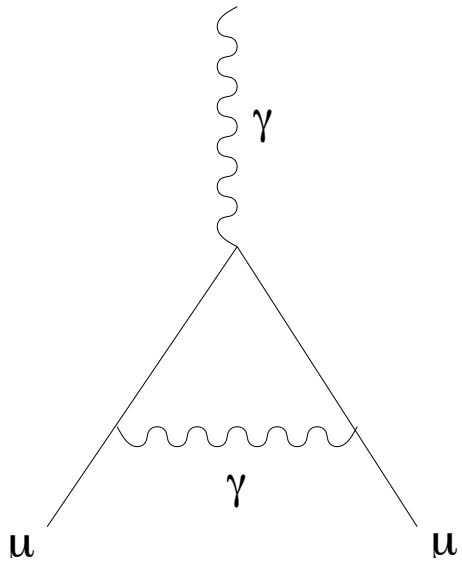

Figure 1: *The first-order QED correction to g-2 of the muon.*

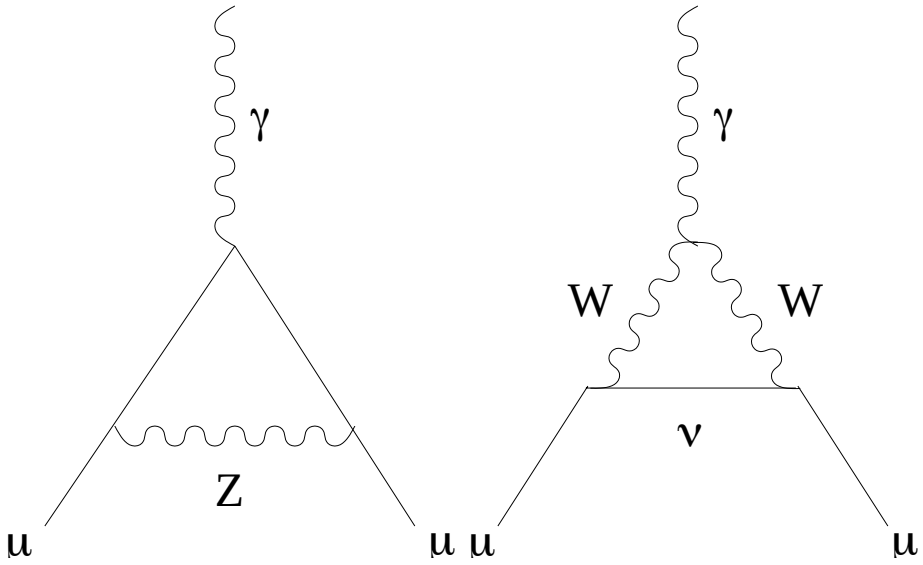

Figure 2: *The two most important first-order electroweak contributions.*

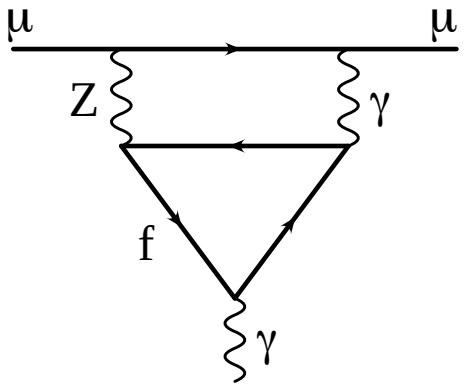

Figure 3: *An example of a 2-loop electroweak contribution (triangle diagram).*

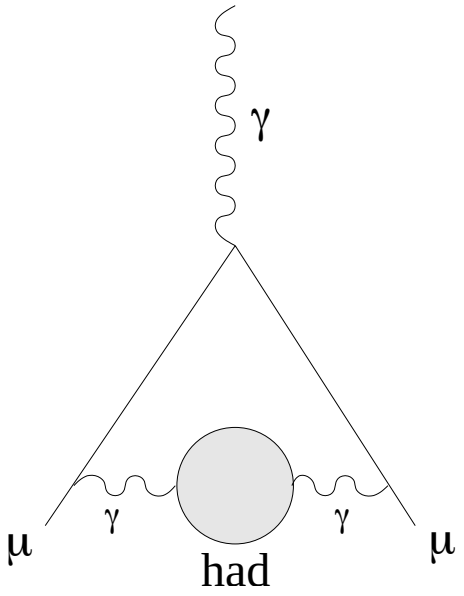

Figure 4: *The lowest-order hadronic contribution.*

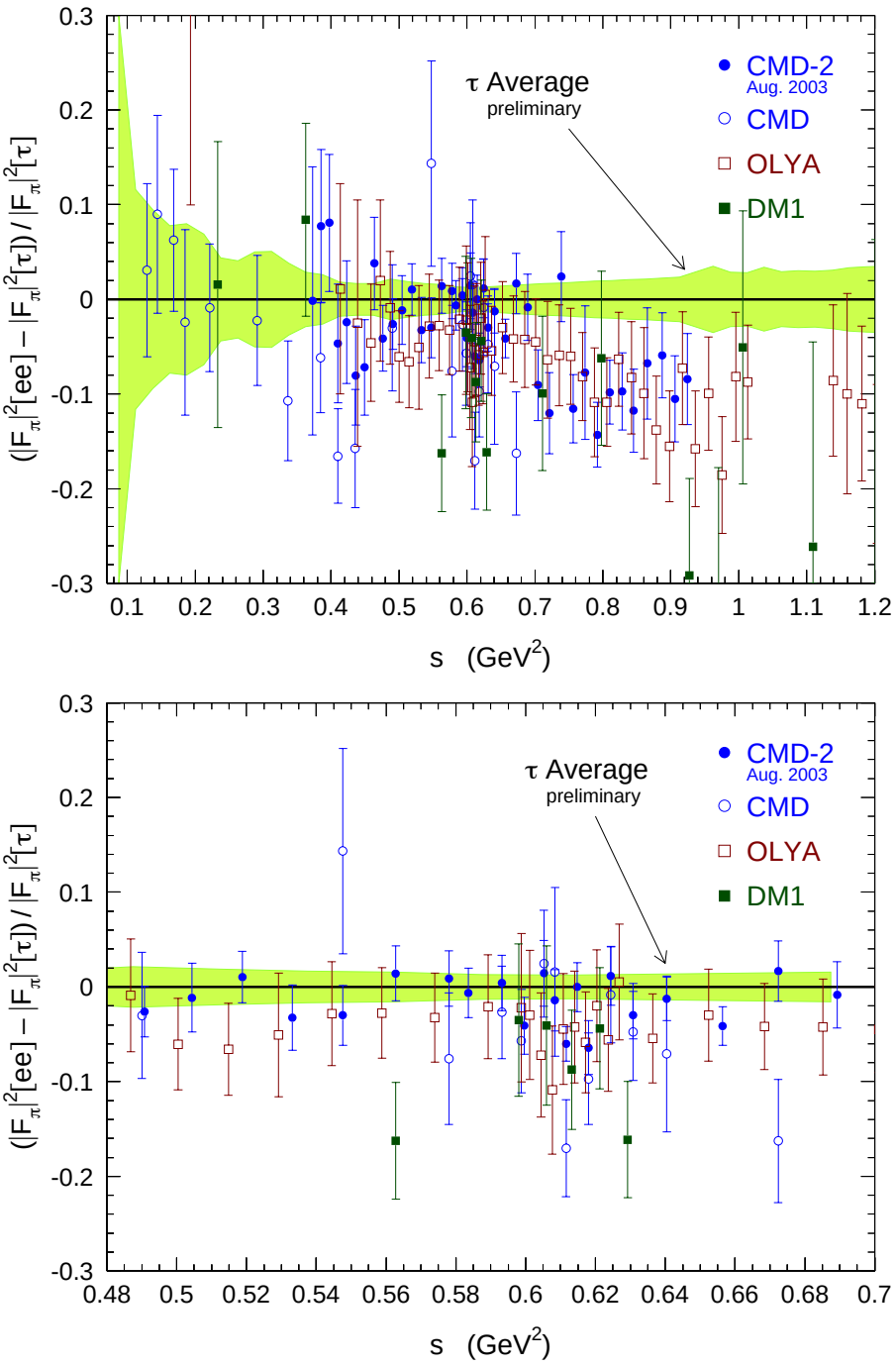

Figure 5: *Relative comparison of the $\pi^+\pi^-$ spectral functions from e^+e^- and isospin-breaking corrected τ data, expressed as a ratio to the τ spectral function. The band shows the uncertainty on the latter. The e^+e^- data are from CMD-2 (33), CMD (54), OLYA (54, 55) and DM1 (56). The bottom plot is an enlargement of the ρ region.*

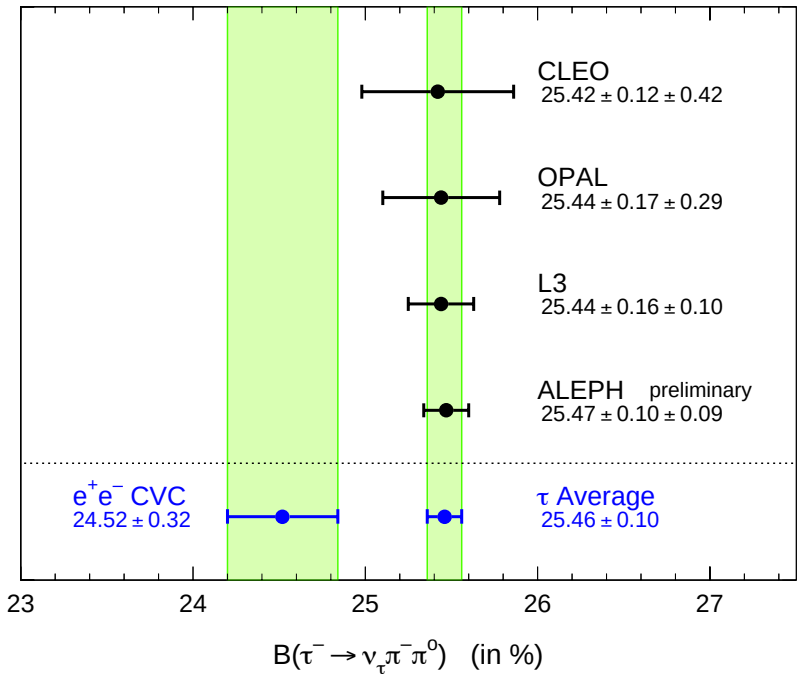

Figure 6: *The measured branching ratios for* $\tau^- \to \nu_\tau \pi^- \pi^0$ *compared to the prediction from the* $e^+e^- \to \pi^+\pi^-$ *spectral function applying the isospin-breaking correction factors discussed in Ref. (32). The measured branching ratios are from ALEPH (42), CLEO (58), L3 (59) and OPAL (60). The L3 and OPAL results are obtained from their* $h\pi^0$ *branching ratio, reduced by the small* $K\pi^0$ *contribution measured by ALEPH (61) and CLEO (62).*

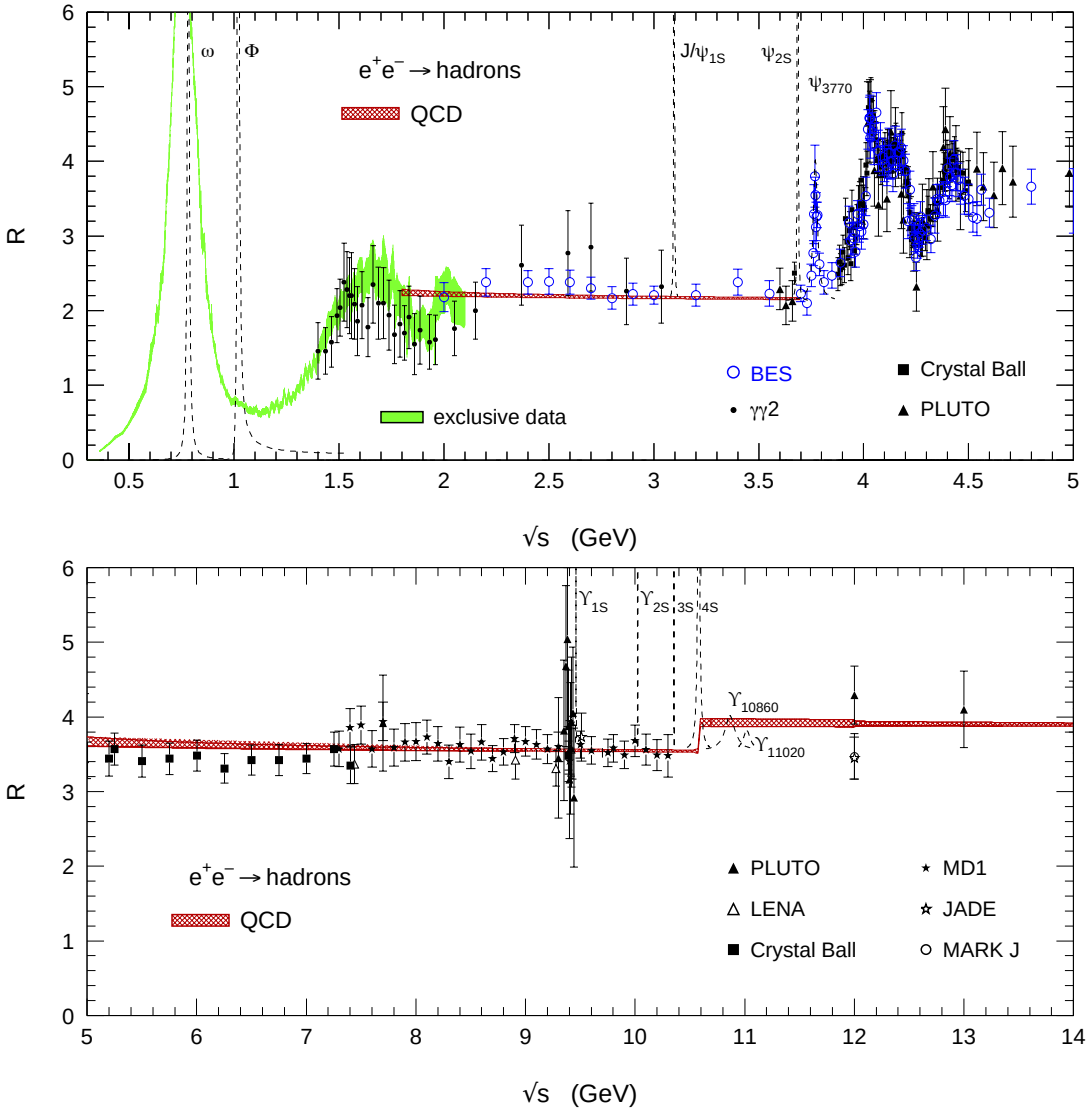

Figure 7: *Compilation of the data contributing to* $a_\mu^{\mathrm{had,LO}}$. *Shown is the total hadronic over muonic cross section ratio* R. *The shaded band below 2 GeV represents the sum of the exclusive channels considered in this analysis, with the exception of the contributions from the narrow resonances which are given as dashed lines. All data points shown correspond to inclusive measurements. The cross-hatched band gives the prediction from (essentially) perturbative QCD (see text).*

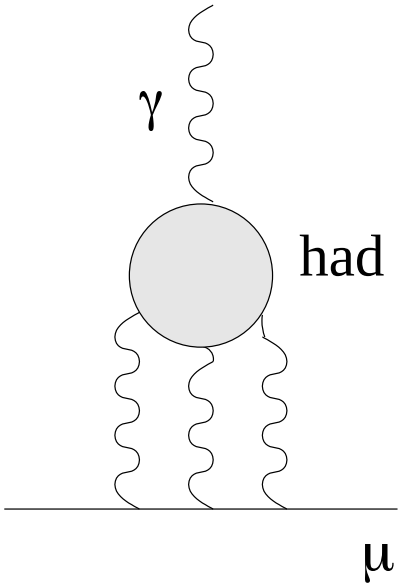

Figure 8: *The hadronic light-by-light scattering contribution.*

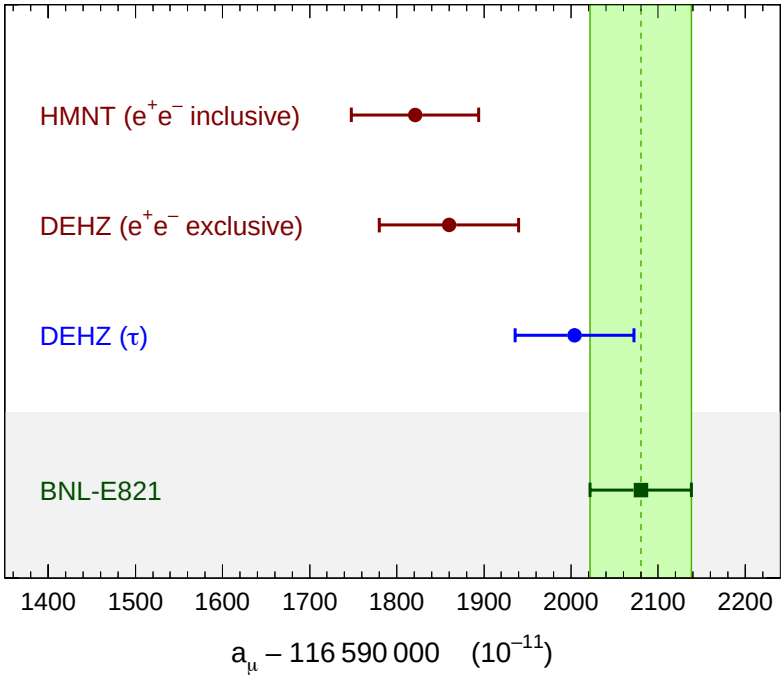

Figure 9: *Comparison of the theoretical estimates (31, 70) with the BNL measurement (13).*

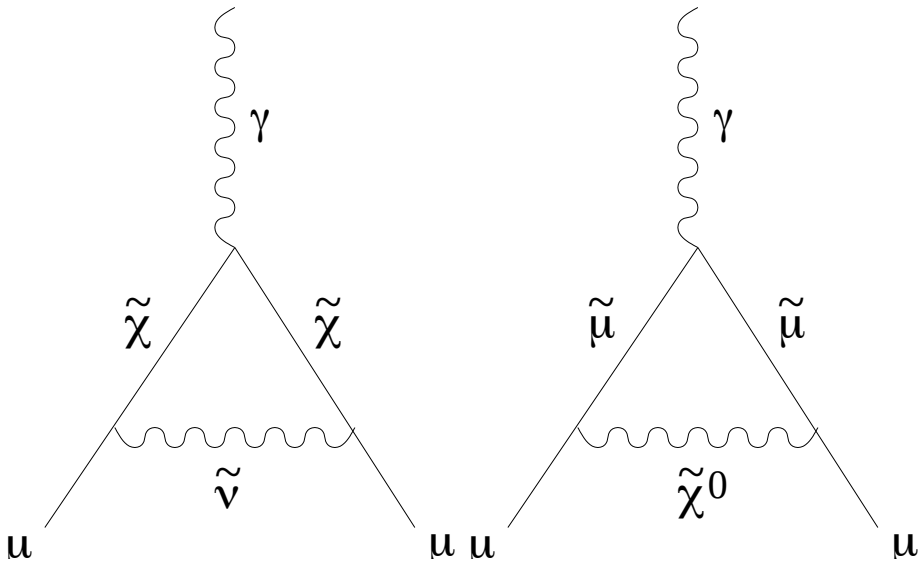

Figure 10: *Two contributions from lowest-order supersymmetry.*